

Supplementary Material

Implementing a distance-based classifier with a quantum interference circuit

M. SCHULD¹, M. FINGERHUTH^{1,2} and F. PETRUCCIONE^{1,3}

¹ *Quantum Research Group, School of Chemistry and Physics, University of KwaZulu-Natal, Durban 4000, South Africa*

² *Maastricht Science Programme, University of Maastricht, 6200 MD Maastricht, The Netherlands*

³ *National Institute for Theoretical Physics, KwaZulu-Natal, Durban 4000, South Africa*

*** Missing PACS ***

Abstract –*** Missing author ***

Estimating the prediction error with confidence intervals. – The prediction result in the quantum circuit is encoded in the probabilities $1 - p = |\alpha|^2$ and $p = |\beta|^2$ to measure the “class qubit” in state $|0\rangle$ or $|1\rangle$ respectively. To get an estimator \hat{p} of the true probability p , we run the algorithm R times to collect a sample of outcomes Q_1, \dots, Q_R . This corresponds to sampling from a Bernoulli distribution of a binary random variable Q with expectation value $\mathbb{E}[Q] = \hat{p}$ and variance $\sigma = \sqrt{\frac{\hat{p}(1-\hat{p})}{R}}$. If $\hat{p} > 0.5$, the result of the classification is 1, while for $\hat{p} < 0.5$ the result is -1 . We want to get an estimate of how the error ϵ we make in choosing this estimator decreases with the sample size R within a sufficiently high confidence level.

A common approach in statistics is to compute a maximum error related to a confidence level z . A z -value of 2.58 corresponds to a confidence level of 99%, which indicates the proportion of confidence intervals around the estimator constructed from different samples in which we expect to find the true value p . Frequently used is the Wald interval which is suited for cases of large R and $\hat{p} \approx 0.5$, which we expect for the classifier due to the broad kernel function. The estimator for p is constructed by maximum likelihood estimation as the average value $\hat{p} = \bar{p} = 1/R \sum_{r=1}^R Q_r$. The maximum error $E = |\bar{p} - p|$ can be determined as

$$E = z\sigma = z\sqrt{\frac{\bar{p}(1-\bar{p})}{R}}.$$

This is maximised for $\bar{p} = 0.5$, so that we can assume the overall error of our estimation ϵ to be at most $\frac{z}{2\sqrt{R}}$ with a confidence level of z . In other words, the number of times we have to repeat the classification algorithm (including state preparation) grows with $\mathcal{O}(\epsilon^{-2})$.

For small sample sizes R , or p close to either zero or one this estimation can fail severely [1]. A more refined alternative is the Wilson score with the following estimator \hat{p} for p ,

$$\hat{p} = \frac{1}{1 + \frac{z^2}{R}} \left(\hat{p} + \frac{z^2}{2R} \right),$$

and the maximum error

$$E = \frac{z}{1 + \frac{z^2}{R}} \left(\frac{\bar{p}(1 - \bar{p})}{R} + \frac{z^2}{4R^2} \right)^{\frac{1}{2}}.$$

Again this is maximised for $\bar{p} = 0.5$ and with a confidence level z we can state that the overall error of our estimation is bounded by

$$\epsilon \leq \sqrt{z^2 \frac{R + z^2}{4R^2}}.$$

27 The more refined estimation yields the same growth with $\mathcal{O}(\epsilon^{-2})$, for all possible estimators
 28 $\bar{p} \in [0, 1]$ (see also [2]).

29 **Details on the experiment with the IBM Quantum Experience.** – At the
 30 time of writing IBM’s quantum processor implements single-qubit gates within 83ns and a
 31 CNOT gate within maximally 483ns [3]. Figure 1 is a schematic drawing showing the cross-
 32 resonance interactions between and the arrangement of the five qubits in the IBM quantum
 33 computer. According to the device calibration results from IBM [4], the amplitude damping
 34 times of the five qubits currently range from 46ms to 61.5ms and the phase damping times
 35 range from 38.6ms to 91.9ms. In the current hardware setup, the maximum single-qubit
 36 error and single-qubit measurement error are 3.3×10^{-3} and 6.4×10^{-2} respectively. As
 37 a result of these qubit errors and decoherence times, the system currently allows for 80
 38 quantum operations per qubit thus enabling 79 quantum gates and one measurement.

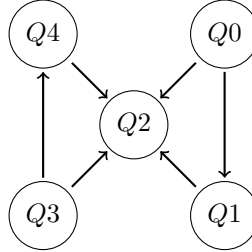


Fig. 1: Schematic drawing illustrating the qubit arrangement and the cross-resonance interactions on the IBM quantum processor chip.

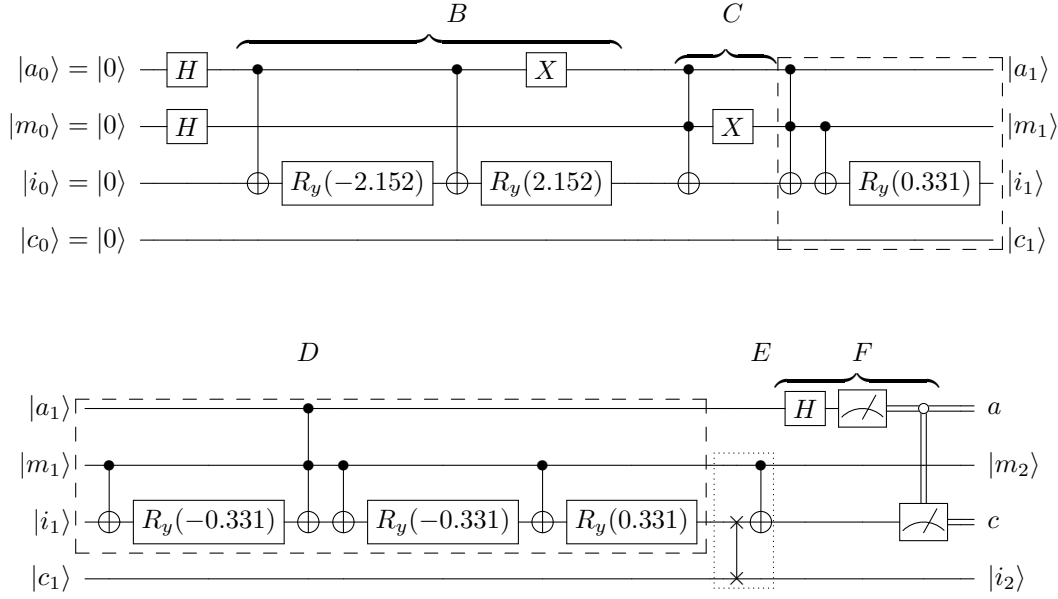


Fig. 2: Quantum circuit with decomposed controlled rotations implementing the distance-based classifier using the two training vectors \mathbf{x}^0 and \mathbf{x}^1 and the input vector $\tilde{\mathbf{x}}'$ from the rescaled and normalised Iris flower dataset. First the input vector is entangled with the ground state of the ancilla (Step B), then the training vector \mathbf{x}^0 is entangled with the excited state of the ancilla and the ground state of the index qubit (Step C) followed by entangling the training vector \mathbf{x}^1 with the excited state of the ancilla and the index qubit (Step D). Finally the data and class qubits are swapped and the class qubit is flipped conditioned on the index qubit being $|1\rangle$ (Step E). In step F after the Hadamard gate the ancilla is measured followed by a measurement of the class qubit when the ancilla was found to be in the $|0\rangle$ state.

The full quantum circuit implementing the classification of input vector $\tilde{\mathbf{x}}'$ is given in Figure 2 where $|a\rangle, |m\rangle, |i\rangle$ and $|c\rangle$ stand for ancilla, index, data and class qubit respectively. Note, that the IBM Quantum Experience (IBMQE) does not provide all-to-all connected CNOT gates which follows directly from the qubit arrangement shown in Figure 1. From Figure 2 it follows that the data qubit $|i\rangle$ is the most frequently used target qubit for controlled operations. The third qubit ($Q2$ in Figure 1) is the only qubit which can be connected to all other qubits by means of CNOT gates and is, thus, chosen to be the data qubit. To flip the class label for the training vector \mathbf{x}^1 a CNOT gate needs to be applied to the class qubit controlled by the index qubit (Step D in Figure 2). The available CNOT connectivity of the IBM quantum computer requires prior swapping of the data and class qubits as indicated in Step D in Figure 2. On the IBMQE a SWAP gate can be implemented with the quantum circuit shown in Figure 3.

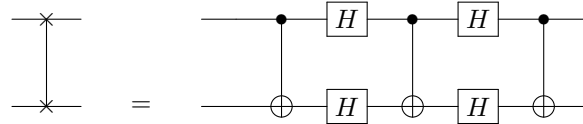


Fig. 3: Quantum circuit implementing a SWAP gate with four Hadamard and three CNOT gates.

The entire quantum state preparation routine outlined in Figure 2 requires the use of three Toffoli gates in Steps B and C. Toffoli gates are not directly supported by the IBM quantum hardware and, thus, need to be decomposed as shown in Figure 4. There are many known ways of decomposing a Toffoli gate but we specifically chose this decomposition since it integrates very well with IBM's CNOT connectivity and has a relatively low T-depth of four.

For the classification of the second input vector $\tilde{\mathbf{x}}''$ the overall quantum circuit shown in Figure 2 remains the same. To load $\tilde{\mathbf{x}}''$ instead of $\tilde{\mathbf{x}}'$ only the rotations in Step A need to be changed to $R_y(-2.152)$ and $R_y(2.152)$ instead of $R_y(-1.518)$ and $R_y(1.518)$.

Table 1 shows the obtained occurrence counts for all four-qubit quantum states after 8192 runs in the classification of input vectors $\tilde{\mathbf{x}}'$ and $\tilde{\mathbf{x}}''$.

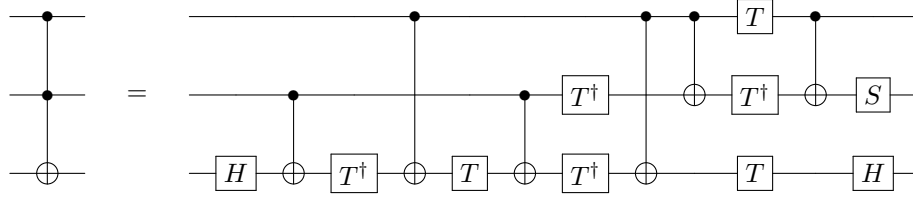


Fig. 4: Quantum circuit implementing a Toffoli gate with ten single-qubit gates (T-depth 4) and six CNOT gates.

	$ 0\rangle$	$ 1\rangle$	$ 2\rangle$	$ 3\rangle$	$ 4\rangle$	$ 5\rangle$	$ 6\rangle$	$ 7\rangle$	$ 8\rangle$	$ 9\rangle$	$ 10\rangle$	$ 11\rangle$	$ 12\rangle$	$ 13\rangle$	$ 14\rangle$	$ 15\rangle$
\mathbf{x}'	773	1400	223	172	210	205	1013	578	823	1175	117	113	95	114	476	705
\mathbf{x}''	948	1117	166	145	155	128	680	626	1139	1136	131	122	127	149	694	729

Table 1: Raw experimental results for the classification of the input vectors $\tilde{\mathbf{x}}'$ and $\tilde{\mathbf{x}}''$. The table shows the occurrence counts for each four-qubit quantum state, $|0000\rangle \rightarrow |0\rangle$, $|0001\rangle \rightarrow |1\rangle$..., in 8192 runs.

REFERENCES

- [1] Lawrence D Brown, T Tony Cai, and Anirban DasGupta. Interval estimation for a binomial proportion. *Statistical Science*, pages 101–117, 2001.
- [2] Ryan Sweke, Mikel Sanz, Ilya Sinayskiy, Francesco Petruccione, and Enrique Solano. Digital quantum simulation of many-body non-markovian dynamics. *Physical Review A*, 94(2):022317, 2016.
- [3] Lev Bishop. Quantum gate times on IBM quantum computer. <https://quantumexperience.ng.bluemix.net/qstage/#/community/question?questionId=71b344418d724f8ec1088bafc75eb334&answerId=3a2f15c989b2aa752f563cfaf53ae240>. Last Accessed December 29, 2016.
- [4] IBM. IBMQE Device Calibration. <https://quantumexperience.ng.bluemix.net/qstage/#/editor>. Last Accessed March 23, 2017.